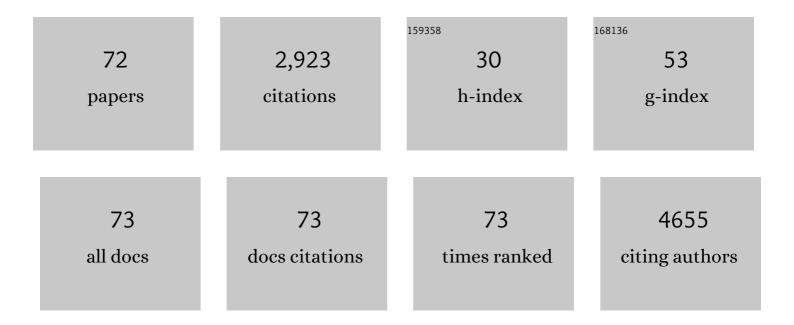
Xiaoyong Xu

List of Publications by Year in descending order

Source: https://exaly.com/author-pdf/5809993/publications.pdf

Version: 2024-02-01



#	ARTICLE	IF	CITATIONS
1	Heteroatomic Platinum–Cobalt Synergetic Active Centers with Charge Polarization Enable Superior Hydrogen Evolution Performance in both Acid and Base Media. ACS Applied Energy Materials, 2022, 5, 1496-1504.	2.5	19
2	Chameleon‣ike Reconstruction on Redox Catalysts Adaptive to Alkali Water Electrolysis. Small, 2022, 18, .	5.2	9
3	Oxygen vacancies activating surface reactivity to favor charge separation and transfer in nanoporous BiVO4 photoanodes. Applied Catalysis B: Environmental, 2021, 281, 119477.	10.8	116
4	Refined Z-scheme charge transfer in facet-selective BiVO4/Au/CdS heterostructure for solar overall water splitting. International Journal of Hydrogen Energy, 2021, 46, 8531-8538.	3.8	23
5	Vertical-orbital band center as an activity descriptor for hydrogen evolution reaction on single-atom-anchored 2D catalysts. Journal of Physics Condensed Matter, 2021, 33, 245201.	0.7	9
6	Role of exchange splitting and ligand-field splitting in tuning the magnetic anisotropy of an individual iridium atom on <mml:math xmlns:mml="http://www.w3.org/1998/Math/MathML"><mml:mrow><mml:mi>Ta</mml:mi><mml:msub><mml:mi mathvariant="normal">S</mml:mi></mml:msub><mml:mn>2</mml:mn></mml:mrow></mml:math>	1.1	17
7	substrate. Physical Review B, 2021, 103, . Pronounced Linewidth Narrowing of Vertical Metallic Split-Ring Resonators via Strong Coupling with Metal Surface. Nanomaterials, 2021, 11, 2194.	1.9	4
8	Engineering Selfâ€Reconstruction via Flexible Components in Layered Double Hydroxides for Superiorâ€Evolving Performance. Small, 2021, 17, e2101671.	5.2	30
9	The mechanism of enhanced photocatalytic activity for water-splitting of ReS ₂ by strain and electric field engineering. RSC Advances, 2021, 11, 23055-23063.	1.7	5
10	MoS ₂ Nanostructures with the 1T Phase for Electromagnetic Wave Absorption. ACS Applied Nano Materials, 2021, 4, 11042-11051.	2.4	29
11	Redox bifunctional activities with optical gain of Ni3S2 nanosheets edged with MoS2 for overall water splitting. Applied Catalysis B: Environmental, 2020, 268, 118435.	10.8	118
12	Photo-induced charge kinetic acceleration in ultrathin layered double hydroxide nanosheets boosts the oxygen evolution reaction. Journal of Materials Chemistry A, 2020, 8, 1105-1112.	5.2	32
13	Plasmonic Cocatalyst with Electric and Thermal Stimuli Boots Solar Hydrogen Evolution. Solar Rrl, 2020, 4, 2070062.	3.1	4
14	Plasmonic Cocatalyst with Electric and Thermal Stimuli Boots Solar Hydrogen Evolution. Solar Rrl, 2020, 4, 2000094.	3.1	11
15	Construction of Active Orbital via Single-Atom Cobalt Anchoring on the Surface of 1T-MoS ₂ Basal Plane toward Efficient Hydrogen Evolution. ACS Applied Energy Materials, 2020, 3, 2315-2322.	2.5	50
16	Organic Dye Molecules Sensitization-Enhanced Photocatalytic Water-Splitting Activity of MoS ₂ from First-Principles Calculations. Journal of Physical Chemistry C, 2020, 124, 6580-6587.	1.5	12
17	Incorporation of active phase in porous MoS2 for enhanced hydrogen evolution reaction. Journal of Materials Science: Materials in Electronics, 2020, 31, 4121-4128.	1.1	3
18	Functionalization of two-dimensional 1T′-ReS ₂ with surface ligands for use as a photocatalyst in the hydrogen evolution reaction: a first-principles calculation study. Physical Chemistry Chemical Physics, 2020, 22, 9415-9423.	1.3	8

XIAOYONG XU

#	Article	IF	CITATIONS
19	Engineering Interfaces to Steer Hole Dynamics of BiVO ₄ Photoanodes for Solar Water Oxidation. Solar Rrl, 2019, 3, 1900115.	3.1	23
20	Transition metal doping activated basal-plane catalytic activity of two-dimensional 1T'-ReS ₂ for hydrogen evolution reaction: a first-principles calculation study. Nanoscale, 2019, 11, 10402-10409.	2.8	56
21	Metallic molybdenum sulfide nanodots as platinum-alternative co-catalysts for photocatalytic hydrogen evolution. Journal of Catalysis, 2019, 374, 237-245.	3.1	37
22	Hole dynamic acceleration over CdSO nanoparticles for high-efficiency solar hydrogen production with urea photolysis. Journal of Materials Chemistry A, 2019, 7, 25650-25656.	5.2	6
23	Identification of few-layer ReS2 as photo-electro integrated catalyst for hydrogen evolution. Nano Energy, 2018, 48, 337-344.	8.2	71
24	Enriching Hot Electrons via NIRâ€Photonâ€Excited Plasmon in WS ₂ @Cu Hybrids for Fullâ€Spectrum Solar Hydrogen Evolution. Advanced Functional Materials, 2018, 28, 1804055.	7.8	89
25	Self-assembly optimization of cadmium/molybdenum sulfide hybrids by cation coordination competition toward extraordinarily efficient photocatalytic hydrogen evolution. Journal of Materials Chemistry A, 2018, 6, 18396-18402.	5.2	22
26	Achieving half-metallicity in zigzag MoS ₂ nanoribbon with a sulfur vacancy by edge passivation. Journal Physics D: Applied Physics, 2018, 51, 265005.	1.3	5
27	Integrating Semiconducting Catalyst of ReS2 Nanosheets into P-Silicon Photocathode for Enhanced Solar Water Reduction. ACS Applied Materials & amp; Interfaces, 2018, 10, 23074-23080.	4.0	30
28	Half-metallic carbon nitride nanosheets with micro grid mode resonance structure for efficient photocatalytic hydrogen evolution. Nature Communications, 2018, 9, 3366.	5.8	219
29	The indirect–direct band gap tuning in armchair MoS ₂ nanoribbon by edge passivation. Journal Physics D: Applied Physics, 2017, 50, 095102.	1.3	20
30	Interface Band Engineering Charge Transfer for 3D MoS ₂ Photoanode to Boost Photoelectrochemical Water Splitting. ACS Sustainable Chemistry and Engineering, 2017, 5, 3829-3836.	3.2	51
31	Creating Carbon–Oxygen Bonds over TiO ₂ Nanofibers for Synergistic Benefits of Visibleâ€Light Response and Charge Separation toward Photocatalysis. Advanced Materials Interfaces, 2017, 4, 1600795.	1.9	6
32	Surface states engineering carbon dots as multi-band light active sensitizers for ZnO nanowire array photoanode to boost solar water splitting. Carbon, 2017, 121, 201-208.	5.4	38
33	Three electron channels toward two types of active sites in MoS ₂ @Pt nanosheets for hydrogen evolution. Journal of Materials Chemistry A, 2017, 5, 22654-22661.	5.2	42
34	Steering Photoelectrons Excited in Carbon Dots into Platinum Cluster Catalyst for Solarâ€Driven Hydrogen Production. Advanced Science, 2017, 4, 1700273.	5.6	39
35	Transition-metal doping induces the transition of electronic and magnetic properties in armchair MoS ₂ nanoribbons. Physical Chemistry Chemical Physics, 2017, 19, 24594-24604.	1.3	24
36	Coexistence of negative photoconductivity and hysteresis in semiconducting graphene. AIP Advances, 2016, 6, .	0.6	14

XIAOYONG XU

#	Article	IF	CITATIONS
37	Two-dimensional ZnO ultrathin nanosheets decorated with Au nanoparticles for effective photocatalysis. Journal of Applied Physics, 2016, 120, .	1.1	23
38	Efficient photon harvesting and charge collection in 3D porous RGO-TiO2 photoanode for solar water splitting. Materials and Design, 2016, 101, 95-101.	3.3	24
39	Enriching Photoelectrons via Three Transition Channels in Amino-Conjugated Carbon Quantum Dots to Boost Photocatalytic Hydrogen Generation. ACS Applied Materials & Interfaces, 2016, 8, 14118-14124.	4.0	57
40	Constructing n-ZnO@Au heterogeneous nanorod arrays on p-Si substrate as efficient photocathode for water splitting. Nanotechnology, 2016, 27, 305403.	1.3	24
41	ZnO quantum dots arranged by hole scavenger groups for enhanced and stable photocatalyic hydrogen generation. Materials Letters, 2016, 165, 196-199.	1.3	10
42	Well–Steered Charge–Carrier Transfer in 3D Branched CuxO/ZnO@Au Heterostructures for Efficient Photocatalytic Hydrogen Evolution. ACS Applied Materials & Interfaces, 2015, 7, 26819-26827.	4.0	77
43	Self-assembled 3D ACF–rGO–TiO2 composite as efficient and recyclable spongy adsorbent for organic dye removal. Materials and Design, 2015, 83, 522-527.	3.3	26
44	Dispersedly embedded loading of Fe ₃ O ₄ nanoparticles into graphene nanosheets for highly efficient and recyclable removal of heavy metal ions. New Journal of Chemistry, 2015, 39, 7355-7362.	1.4	30
45	Photogenerated electron reservoir in hetero-p–n CuO–ZnO nanocomposite device for visible-light-driven photocatalytic reduction of aqueous Cr(<scp>vi</scp>). Journal of Materials Chemistry A, 2015, 3, 1199-1207.	5.2	231
46	Room Temperature Ferromagnetism and Photoluminescence in Cu-Doped ZnO Nanocrystals. Journal of Nanoscience and Nanotechnology, 2014, 14, 6012-6015.	0.9	5
47	High-performance deep ultraviolet photodetectors based on ZnO quantum dot assemblies. Journal of Applied Physics, 2014, 116, .	1.1	26
48	Manganese ion-assisted assembly of superparamagnetic graphene oxide microbowls. Applied Physics Letters, 2014, 104, 121602.	1.5	2
49	Resistive switching memories in MoS2 nanosphere assemblies. Applied Physics Letters, 2014, 104, .	1.5	62
50	Vertically aligned MoS ₂ /MoO _x heterojunction nanosheets for enhanced visible-light photocatalytic activity and photostability. CrystEngComm, 2014, 16, 9025-9032.	1.3	58
51	Photoanode Current of Large–Area MoS ₂ Ultrathin Nanosheets with Vertically Mesh–Shaped Structure on Indium Tin Oxide. ACS Applied Materials & Interfaces, 2014, 6, 5983-5987.	4.0	79
52	Photogenerated Carriers Transfer in Dye–Graphene–SnO ₂ Composites for Highly Efficient Visible-Light Photocatalysis. ACS Applied Materials & Interfaces, 2014, 6, 613-621.	4.0	122
53	Transparent SnO2 QDs-based multifunctional glass for ultraviolet-blocking and enhanced hydrophobicity. Materials Letters, 2014, 128, 291-294.	1.3	10
54	Comparison on Photoluminescence and Magnetism between Two Kinds of Undoped ZnO Nanorods. Journal of Physical Chemistry C, 2013, 117, 24549-24553.	1.5	44

XIAOYONG XU

#	Article	IF	CITATIONS
55	Localized Surface Plasmon Resonanceâ€Enhanced Twoâ€Photon Excited Ultraviolet Emission of Auâ€Decorated ZnO Nanorod Arrays. Advanced Optical Materials, 2013, 1, 940-945.	3.6	33
56	Transparent and UV-shielding ZnO@PMMA nanocomposite films. Optical Materials, 2013, 36, 169-172.	1.7	88
57	PEGME-bonded SnO2 quantum dots for excellent photocatalytic activity. RSC Advances, 2013, 3, 20422.	1.7	19
58	Controllable fabrication and optical properties of Sn-doped ZnO hexagonal microdisk for whispering gallery mode microlaser. APL Materials, 2013, 1, .	2.2	18
59	Control mechanism behind broad fluorescence from violet to orange in ZnO quantum dots. CrystEngComm, 2013, 15, 977-981.	1.3	39
60	Variation of structural, optical and magnetic properties with Co-doping in Sn1â^'xCoxO2 nanoparticles. Journal of Magnetism and Magnetic Materials, 2013, 327, 24-27.	1.0	35
61	Single ZnO Microrod Ultraviolet Photodetector with High Photocurrent Gain. ACS Applied Materials & Interfaces, 2013, 5, 9344-9348.	4.0	101
62	Brush-like SnO2/ZnO hierarchical nanostructure: Synthesis, characterization and application in UV photoresponse. AIP Advances, 2013, 3, .	0.6	24
63	Role of zinc vacancies in driving ferromagnetism in undoped ZnO granular films. Europhysics Letters, 2013, 101, 27009.	0.7	13
64	DEFECT-ORIGIN AND STABILITY OF VISIBLE EMISSION IN ZnO NANOPILLARS. Functional Materials Letters, 2012, 05, 1240001.	0.7	7
65	Structure evolution and optical properties of hierarchical ZnO micro/nanorods fabricated by a two-step growth method. CrystEngComm, 2012, 14, 2180.	1.3	4
66	Surface photoluminescence and magnetism in hydrothermally grown undoped ZnO nanorod arrays. Applied Physics Letters, 2012, 100, 172401.	1.5	41
67	Size Dependence of Defect-Induced Room Temperature Ferromagnetism in Undoped ZnO Nanoparticles. Journal of Physical Chemistry C, 2012, 116, 8813-8818.	1.5	201
68	Identification of visible emission from ZnO quantum dots: Excitation-dependence and size-dependence. Journal of Applied Physics, 2012, 111, 083521.	1.1	40
69	Evolutions of defects and blue–green emissions in ZnO microwhiskers fabricated by vapor-phase transport. Journal of Physics and Chemistry of Solids, 2012, 73, 858-862.	1.9	32
70	Excitation-dependent photoluminescence of ZnO microrods with MgO surface coating. Materials Letters, 2012, 82, 145-147.	1.3	6
71	Strain-induced magnetoresistance for novel strain sensors. Journal of Applied Physics, 2010, 108, 033916.	1.1	7
72	The cooling field and the exchange bias in ferromagnet/antiferromagnet bilayers. Journal of Applied Physics, 2009, 106, .	1.1	14